Journal of Physical and Theoretical Chemistry
of Islamic Azad University of Iran, 17 (3, 4) 107-122: Fall 2020 & Winter 2021
(J. Phys. Theor. Chem. IAU Iran)
ISSN 1735-2126

The interaction of 5-Flucytosine drug with pristine and (*n=1, 2, 3*) H^+ ions functionalized B12N12 nanocage: A DFT, TD-DFT, NLO and AIM study

M. Rezaei-Sameti* and S. Doosti Tapehkaboodi

Department of Applied Chemistry, Faculty of Science, Malayer University, Malayer, 65174, Iran

Received July 2020; Accepted January 2020

ABSTRACT

The aims this work to investigate the effects of (*n*=1, 2, 3) H+ ions functionalizing on the surface of B12N12 nanocage to detect and adsorb 5-Flucytosine (5-FC) drug using density functional theory at the WB97XD/6-31G(d, p) level of theory using Gaussian 09 software. The calculated results indicate that the adsorption of 5-FC drug on the surface of pristine and nH$^+$ functionalized B12N12 nanocage is exothermic, and adsorption process in the presence of nH$^+$ functionalized is more favorable than the pristine model. The thermodynamic results demonstrate that the adsorption of 5-FC on the surface of nH$^+$ functionalized B12N12 nanocage in both the gaseous phase and in the presence of water or ethanol is spontaneous. The gap energy value of nH$^+$ functionalized of B12N12 nanocage is more than the original value and so the conductivity of the system is lower than the pristine model. The AIM and RDG results confirm that the interaction between 5-FC with B12N12 is noncovalent type. The nonlinear optical (NLO) results show that the polarizability (α) and hyperpolarizability (β) of all adsorption models is in range (202.30 to 214.34 a.u.) and (42.18 to 603.98 a.u.) respectively, the NLO and TD-DFT results demonstrate that the optical properties of nanocage in the presence of 5-FC drug and nH$^+$ functionalized change significantly. These results can be useful for making carrier, delivery, and detection of drugs in the biological system.

Keywords: $B_{12}N_{12}$ nanocage; nH$^+$ functionalized; DFT; Flucytosine drug; AIM

1. INTRODUCTION

Over the years, extensive efforts have been made on a variety of nanoparticles, including nanotubes, nanosheets, and nanocages. The electrical, structural, stability and optical properties of these nanomaterials have studied in various fields such as drug design, nanoelectronic devices, and chemical sensors various toxic materials [1–5]. One of the most prominent of this nanomaterial is boron nitride nanocage $(BN)_{12}$. Oku *et al.* for the first time was successfully synthesized $(BN)_{12}$ through laser desorption time-of-flight mass spectrometry [6]. The

*Corresponding author: mrsameti@gmail.com, mrsameti@malayeru.ac.ir

theoretical results demonstrated that the formation energy of the $(BN)_{12}$ nanocage is −298.3 kcal/mol, it is energetically favorable among other $(BN)_n$ nanocage series and it consists of eight hexagonal six and tetragonal ring [7]. The previous investigations demonstrated that the $(BN)_{12}$ nanocages have outstanding properties in the electrical, optical, magnetic, nanosensors, and nano adsorbent materials, batteries, and nano-drug delivery [8–12].

Yourdkhani *et al*. [13] indicated that the electronic structure properties of $(BN)_{12}$ are very sensitive to the HX (X=Cl, Br, and I) adsorption, and the impurities greatly improve their physicochemical properties. Wu et al. [14], Zhao *et al*. [15], and Esrafili [16–17] revealed that the C-doped increased the sensitivity of $(BN)_{12}$ to adsorbing hydrogenation, hydrochlorination of acetylene, methanol dehydrogenation and Formic acid respectively. Other reports demonstrated that the pristine and doped $(BN)_{12}$ nanocages are useful for adsorption of several important molecules such as: Formaldehyde [18], Halomethanes [19], NH_3 [20], CO [21], CO_2 [22], (N_2, NO, N_2O and NO_2) [23], Tabun [24], SO_2 [25], Thiophene [26], Phosgene [27], Formaldehyde [28], Hydrogen cyanide [29], H_2S [30], Noble gas [31], Cyanogen halides [32], H_2 [33], Hydrogen abstraction of methanimine [34], Methanol [35], SCN^- [36].

Another use of boron nitride nanocage is as a drug carrier in the pharmaceutical industry. Various studies have been carried out for this purpose, including Ghasemi *et al*. [37] results indicated that with interacting 1-butyl-4-methyl pyridinium bromide ionic liquid with B12N12 nano-cage, the sensitivity and value of dipole moment of nanocage increased significantly from pure values.

The calculated results of Farmanzadeh et *al*. [38] showed that the amantadine drug molecule can be adsorbed chemically on the surfaces of pristine and Al-doped B12N12 nanocage in both gas phase and water media. Padash et *al*. [39] results demonstrated that the 4-aminopyridine drug boned from the nucleophilic part of drug on the the electrophilic part of B12N12 nanocage and the adsorption energy was −1.35 eV. The results of Zhu et al [40] confirmed that the adsorption of 5-aminosalicylic acid drug energetically on the surface of pristine B12N12 nanocage was more favorable sensitive than AlB11N12 and GaB11N12 nanocage, and the recovery time of adsorption on the surface of B12N12 nanocage is 1.57 second at 298 K. Baei [41] found that the B12N12 nanocage was highly sensitive to adenine, uracil, and cytosine compared with Al12N12 to serve as a biochemical sensor. The results of Bahrami *et al*. showed that amphetamine drug prefers to adsorb via its nitrogen atom on the Lewis acid sites of the B12N12 nano-cages, and the conductivity of system change significantly from pure state [42].

Larkia et al. [43] results showed that with adsorbing pnictogen hydrides onto the Al-, Ga- and Sc-doped B12N12 nanocage the gap energy increase, which can produce an electrical signal.

One of the oldest antifungal agents and antifungal medication is 5-Fluorocytosine (5-FC), a fluorinated analog of cytosine. 5-FC was synthesized in 1957, as a potential anti-tumor agent, an antifungal medication [44] but it was not sufficiently effective against tumors [45]. Four years later, 5-FC proved to be active in experimental candidosis and cryptococcosis in mice [46], and in 1968, it was used to treat human candidosis and cryptococcosis [47]. One of the new and promising therapeutic approaches that take advantage of the effectiveness of 5-FC and minimizes its systemic toxicity is the use of an enzyme/prodrug combination in which 5-

FC is combined with an Escherichia coli gene that encodes the enzyme cytosine deaminase [48]. It is hoped that this combination will deliver high local concentrations of 5-FC at the tumor site.

In this work, we decided to investigate the interaction 5-FC with the pristine and $1H^+$, $2H^+$ and $3H^+$ ions functionalized B12N12 nanocage. The structural, electrical properties, thermodynamic parameters, atom in molecule topology, nonlinear optical property, and effect of solvent (water and ethanol) are calculated using density functional theory. The results of this work can be used to predict the sensitivity of B12N12 nanocage to detect or delivery and carrier 5-FC drug in the biological system.

2. COMPUTATIONAL DETAILS

In this work, we considered different configurations for adsorption of 5-FC drug on the surface of the pristine, $1H^+$, $2H^+$, and $3H^+$ functionalized boron nitride nanocluster. After optimizing all structures, the suitable configurations are selected. The selected configurations are fully optimized at the WB97XD/6-31G (d, p) level of theory using the Gaussian 09 package [49]. The optimization criteria for systems are: Max force= 0.00044; RMS force= 0.0003; Max. Displacement = 0.0018 and RMS displacement= 0.0012. No imaginary frequency is seen for all studied configurations. For simplicity our study, the pristine, $1H^+$, $2H^+$ and $3H^+$ functionalized B12N12 nanocage is denoted with A, B, C and D labels, the indexes **a**, **b**, **c,** and **d** are used to denote the adsorption positions of 5-FC molecule from F, NH_2, O and NH sites on the surface of nanocage (See Figs. 1 and 2).

From optimized structures the adsorption and thermodynamic parameters for adsorbing 5-FC molecule on the surface of the pristine and H^+ functionalized B12N12 nanocage is calculated by Eqs. 1 and 2:

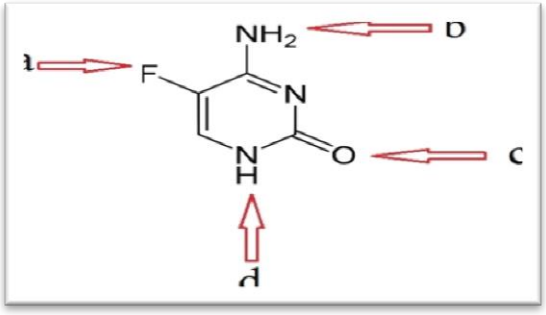

Fig. 1. Adsorption positions of 5- FC drug.

$$E_{ads} = E_{5-FC/(B12N12\,or\,nH^+B12N12)} - (E_{(B12N12\,or\,nH^+B12N12)} + E_{5-FC}) \quad (1)$$

$$\Delta K = K_{5-FC/(B12N12\,or\,nH^+B12N12)} - (K_{(B12N12\,or\,nH^+B12N12)} + K_{5-FC}) \quad K = H, G, S \quad (2)$$

In Eq. 1 the $E_{5-FC/(B12N12\ or\ nH^+B12N12)}$, $E_{(B12N12\,or\ nH^+B12N12)}$ and E_{5-FC} is the total electronic energy of the 5-FC/(B12N12 or nH$^+$B12N12) complexes (A−a to D−c adsorption models). The $E_{(B12N12\,or\ nH^+B12N12)}$, and E_{5-FC} are total electronic energy of the isolated nanocage (B12N12 or H^+B12N12 or $2H^+$B12N12 or $3H^+$B12N12) and isolated 5-FC drug respectively. The thermodynamic parameters such as ΔH, ΔS, ΔG for all

adsorption models (A-a to D-c models) are calculated by Eq. 2, and the calculated results are listed in Table 1.

From the HOMO (highest occupied molecular orbital) and the LUMO (lowest unoccupied molecular orbital) energies, the gap energy (E_{gap}), the ionization potential ($I= -E_{HOMO}$), the electron affinity of the molecule ($A= -E_{LUMO}$), Fermi level energy (E_{FL}), electronic chemical potential (μ), global hardness(η), electronegativity (χ), work function (φ) and charge transfer parameters [50−55] of the A−a to D−c models were calculated by Eqs.(3−8) and results are gathered in Table 2.

$$E_{gap} = E_{LUMO} - E_{HOMO} \quad (3)$$

$$\mu = -(I + A)/2 \quad (4)$$

$$\eta = (I - A)/2 \quad (5)$$

$$\chi = -\mu \quad (6)$$

$$\Delta N = -\mu/\eta \quad (7)$$

$$E_{FL} = (E_{HOMO} + E_{LUMO})/2 \quad (8)$$

The mean polarizability (α_o) and first hyperpolarizability (β_o) are defined as by Eqs. (9−10) [56]:

$$\alpha_0 = \frac{1}{3}(\alpha_{xx} + \alpha_{yy} + \alpha_{zz}) \quad (9)$$

$$\beta_0 = (\beta_x^2 + \beta_y^2 + \beta_z^2)^{0.5} \quad (10)$$

3. RESULTS AND DISCUSSIONS

3.1 Geometrical properties and adsorption parameters

The optimized structures of the A-a to D-d adsorption models are shown in Figure 2 and Figures S1 and S2 (in the supplementary data). According to the optimized results, the B–N bonds between two 6-membered rings and between a 4-membered and a 6-membered of B12N12 nanocage are 1.44 and 1.48 Å respectively, which are in good agreement with other related research [57−58].

Comparison of the A-a to D-d adsorption models indicate that with adsorbing 5-FC on the B site of pristine, $1H^+$, $2H^{+,}$ and $3H^+$ functionalized B12N12, the B−N bonds between two 6-membered rings and between a 4-membered and a 6-membered alter slightly from the original state. The bond distance ($d_{5\text{-FC-nanocage}}$) and the bond angle between the 5-FC drug and nanocage are shown in Figure 2. The obtained results reveal that the $d_{5\text{-FC-nanocage}}$ of the B-a (3.79 Å) and D-c (1.44 Å) models are more and lower than other models. The bond angle between 5-FC and nanocage is in range 79.08 to 159.85 ^{o}. The adsorption energy is calculated by Eq. 1 and the results are listed in Table 1.

The results of adsorption energy show that in all adsorption models, the adsorption process is exothermic and the adsorption takes place between the drug and the B12N12 nanocage.

Interestingly, 5-FC drug uptake from the **c** position (i.e., oxygen head) on the nanocage is greater and more favorable than all adsorption states. While, the adsorption of the 5-FC drug from the **b** position (i.e., −NH) on the surface of

nanocage is lower than other adsorption models. A closer look at the adsorption energy results shows that with functionalizing *n*H+ ion, the intensity of adsorption of 5-FC drug on the surface of B12N12 nanocage increases. As the amount of H^+ ions increases, more energy is released and the absorption process becomes more favorable. The order of increasing adsorption of 5-FC drugs in different drug positions on the surface of pristine B12N12 nanocage is as follows: **c** (−37.46 kcal/mol)> **d** (−12.37 kcal/mol)>**a** (−10.31 kcal/mol) >**b**(−5.17 kcal/mol). While by functionalizing $1H^+$ ions, the order of increasing the absolute value of adsorption energy is as follows: **B-c**(−71.54 kcal/mol) > **B-b**(−46.38

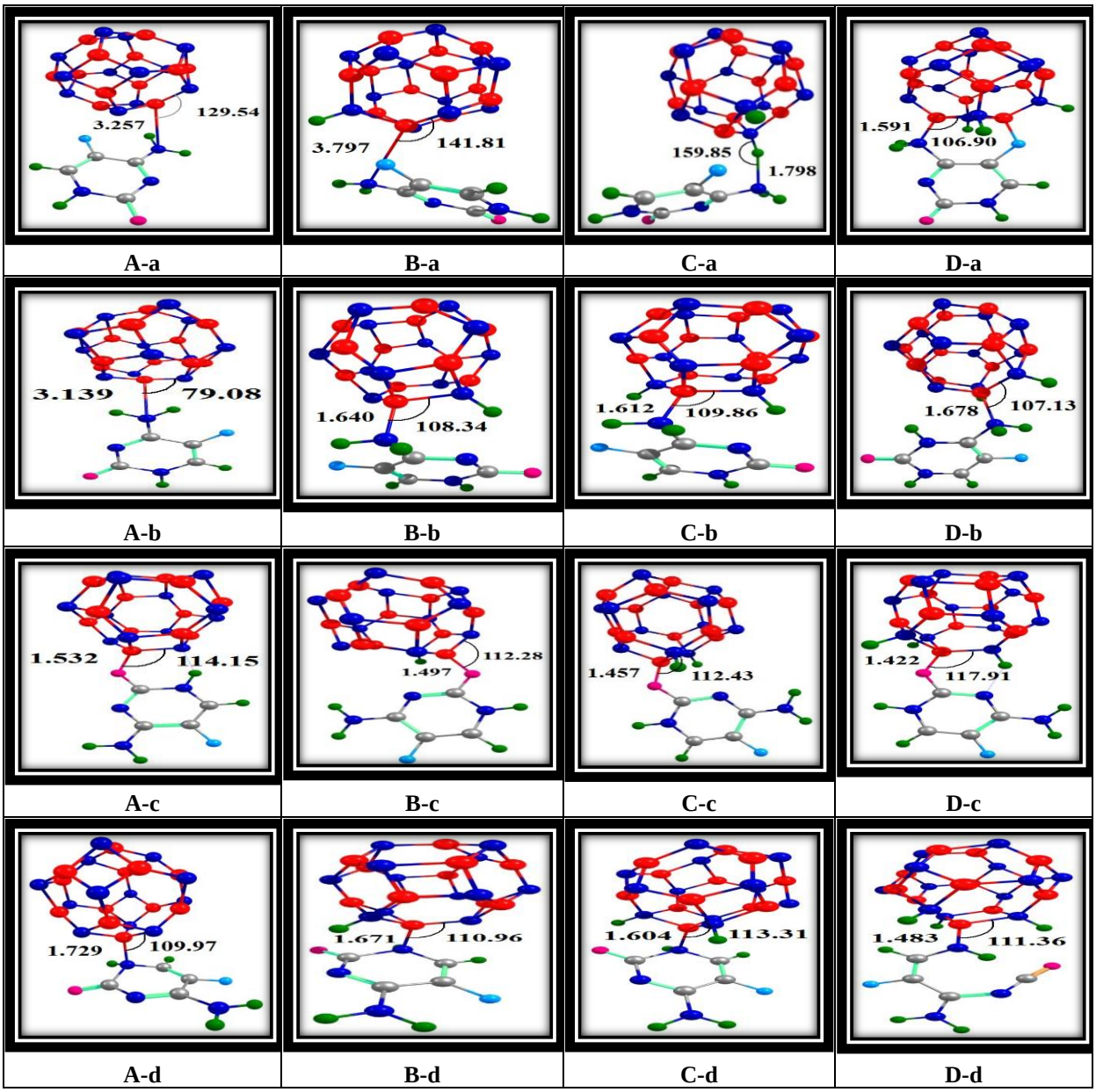

Fig. 2. 2D views of 5-FC adsorption on the surface of pristine and $1H^+$, $2H^+$ and $3H^+$ ions functionalized B12N12 nanocage (A-a to D-d), models.

Table 1. Adsorption energy (E_{ads} (Kcal/mol)), thermodynamic parameters (ΔG, ΔH (Kcal/mol) and ΔS (Cal/mol.K) and Gibbs free energy ΔΔG (Kcal/mol) in water (W) and ethanol (Et) solvent of B12N12/5-FC complex for A-a to D-c models

Model	E_{ads}	ΔH	ΔS	ΔG	$\Delta\Delta G_{(W)}$	$\Delta\Delta G_{(Et)}$
A-a	-10.31	-8.58	-38.11	2.78	4.25	4.34
B-a	-13.41	-35.34	-47.27	-21.24	-7.31	-3.77
C-a	-40.26	-38.99	-46.23	-24.88	-5.40	-5.47
D-a	-105.51	-102.30	-50.24	-87.33	-79.72	-82.87
A-b	-5.17	-3.38	-32.39	6.27	7.70	7.82
B-b	-46.38	-43.87	-46.58	-29.79	-34.86	-23.98
C-b	-75.55	-72.53	-61.00	-58.75	-37.18	-37.58
D-b	-142.79	-138.23	-47.77	-123.99	-82.59	-83.52
A-c	-37.46	-35.97	-47.24	21.89	24.34	23.93
B-c	-71.54	-69.57	-46.00	-55.68	-56.25	-45.79
C-c	-118.49	-85.86	-46.35	-72.04	-68.66	-69.70
D-c	-186.54	-182.38	-49.40	-167.64	-102.09	-104.41
A-d	-12.37	-10.59	-46.81	3.36	4.51	3.06
B-d	-33.11	-31.32	-46.00	-17.60	-19.35	-9.38
C-d	-68.53	-66.31	-46.35	-52.48	-20.40	-25.98
D-d	-140.28	-138.54	-39.08	-123.36	-62.05	-63.70

kcal/mol)>**B-d**(−33.11 kcal/mol)>**B-a** (−13.41 kcal/mol), and the order of increasing the absolute value of the adsorption energy of 5-FC on the surface of nanocage with the number of H^+ ions is as follows: **D**($3H^+$ ion)> **C**($2H^+$ ion)>**B**(H^+ ion)>**A**(pristine). Our calculation results prove that by functionalizing H^+ ions on the surface of B12N12 nanocage, the adsorption process of 5-FC drug on the nanocage becomes more favorable, and the nanocage functionalized is a good option for drug carrier. Thermodynamic parameters such as ΔH, ΔG, ΔS are calculated using Eq. 2 and the calculatedresults are collected in Table 1. Inspection of thermodynamic results indicates that the values of change enthalpy and entropy are negative in all adsorption models and indicates that a bond has occurred between the drug and the nanocage. Interestingly, the trend of enthalpy change results is the same as that of adsorption energy. On the other hand, it can be seen that the change of Gibbs free values for adsorption of 5-FC on the surface of pristine B12N12 nanocage (A-a, A-b, A-c and A-d models) are positive and adsorption process is non-spontaneous. However, by functionalizing H^+ ions, the change of Gibbs free energy is negative and the adsorption process becomes more spontaneous. The polarizable continuum model (PCM) method [59] has been used to investigate the solvent effect on the adsorption of 5-FC drug on the surface of pristine and nH^+ functionalized B12N12 nanocage. The PCM is a useful theoretical method for understanding of all solute-solvent interactions. By using PCM method the effects of water and ethanol effects on the Gibbs free energy of the system ($\Delta\Delta G_{(sol)}=\Delta G_{(sol)FC/B12N12}-\Delta G_{(sol)(FC)}-\Delta G_{(sol)(B12N12)}$) is calculated and results are listed in Table 1. Inspection of the solvent (water or ethanol) effect results reveal that the adsorption process of 5-FC drug on the surface of pristine B12N12 is unspontaneous, because the $\Delta\Delta G_{(sol)}$ values for A-a, A-b, A-c and A-d models are positive. However, in the nH^+ functionalized models with entering water or ethanol, the adsorption process is spontaneous. A comparison of the results demonstrates that the adsorption process of 5-FC drug on the surface of nH^+

functionalized B12N12 nanocage is spontaneous both in the gaseous phase and in the presence of water or ethanol phase. These results confirm that the stability of 5-FC/B12N12 and 5-FC/*n*H^+B12N12 complexes reduce in the solution phase. On the other hand, functionalizing B12N12 nanocage with *n*H^+ ions is a good candidate for connecting 5-FC drug to the nanocage and delivery of it in biological systems.

3.2 Quantum parameters

For investigating the electrical properties of the adsorption 5-FC on the surface pristine and *n*H+ functionalized B12N12 the HOMO and LUMO orbital and other quantum parameters such as gap energy (E_{gap}), global hardness (η), electrochemical potential (μ), electronegativity(χ), Fermi level energy(E_{FL}), work function, total charge transfer parameters(ΔN), the density of state (DOS) and partial density of state (PDOS) are calculated and results are given in Table 2 and shown in Figs.(3, 4 and S3). As shown in Figure 2, the highest density of HOMO orbitals in all adsorption models is concentrated on the drug surface, while the highest density of LUMO orbitals in the A-a, D-a, B-b, C-b, and C-c models are localized on the drug and in the B-a, C-a, D-b, A-c, B-c and D-c models are concentrated around B12N12 nanocage.

In the A-b model, the highest density of LUMO orbital is localized around the surface of the drug and nanocage. From HOMO and LUMO results the density of states (DOS) and partial densities of states (PDOS) of all atoms in range −5 to 25 eV for the A-a to D-c adsorption models are determined and results are shown in Figures 4, and S3 (in supplementary data).

Based on the results of Figure 4, it can be seen that in the A-a model, the amount of PDOS oxygen atom of drug and nitrogen atom of nanocage is higher than other atoms. On the other hand, in the HOMO and LUMO areas, there is the greatest overlap between the 2P and 3P orbitals of the drug oxygen and the nanocage nitrogen respectively, and this interaction is good for bonding between drug and nanocage. In the B-a model, it is observed that by functionalizing $1H^+$ ion, the intensity of the PDOS peaks of **F** atom in the HOMO and LUMO regions are the highest. Interestingly, between orbital 2P of **N** and **F** atoms of drug with 1S orbital of H^+, the most interactions are shown, and in the LUMO region, the most overlap is shown between 3P orbital of **N** and **F** atoms of drug and 3P orbital of **B** atom. In the C-a model, the intensity of the PDOS peak of **N** atom of nanocage and **C** atom of the drug in the HOMO and LUMO regions is the highest. In the HOMO and LUMO regions between orbital 2P of **N**-nano, **N**-drug, and **C** atoms are the highest. And in the LUMO region, the most overlap is shown between 3P orbital of **N**-drug, **N**-nano, and **B** atoms.

In the D-a model, the intensity of the PDOS peaks of C atom of the drug in the HOMO and LUMO regions are the highest. In the HOMO region between 2P orbital of **C**, **N**-nano and **N**-drug atoms are shown the most interaction, whereas in the LUMO region the most interaction is shown between 3P orbital of **C**, **N**-nano, and **N**-drug atoms.

Based on the results of Table 2, the energy level of HOMO and LUMO of B12N12 nanocage decreases with functionalizing *n*H^+ ions, and it is interesting to note that with an increasing number of hydrogen ions, the amount of HOMO and LUMO energy more decrease. The gap energy of the pristine, $1H^+$, $2H^+$ and $3H^+$ functionalized B12N12 are 11.13, 10.20, 9.32 and 7.41 eV, respectively (see Table S1).

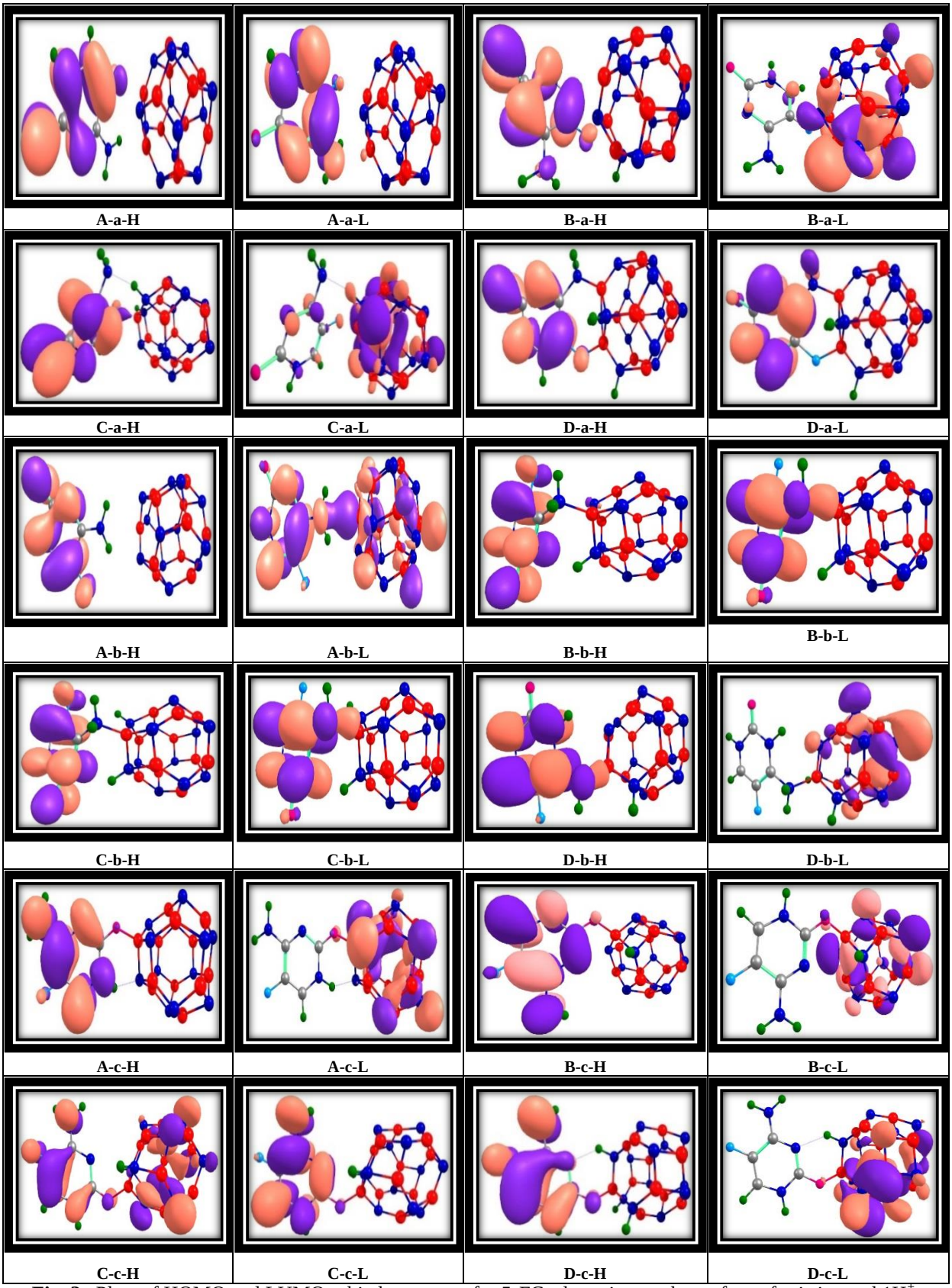

Fig. 3. Plots of HOMO and LUMO orbital structures for 5-FC adsorption on the surface of pristine and $1H^+$, $2H^+$ and $3H^+$ ions functionalized B12N12 nanocage (A-a to D-d), models.

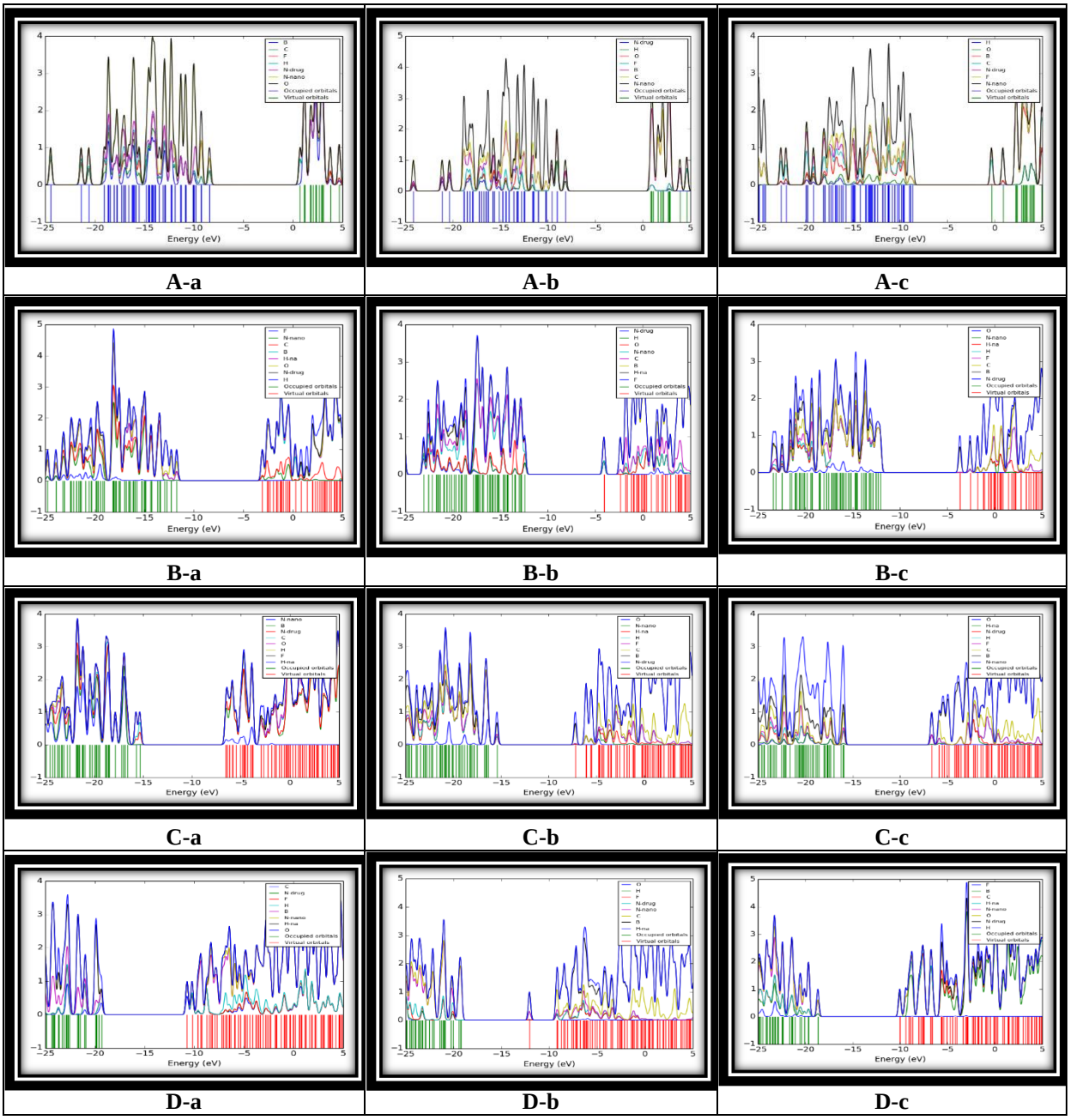

Fig. 4. PDOS plots of 5-FC adsorption on the surface of pristine and $1H^+$, $2H^+$ and $3H^+$ ions functionalized B12N12 nanocage (A-a to D-d), models.

Table 2. The quantum parameters B12N12/5-FC complex for A-a to D-c models

	A-a	B-a	C-a	D-a	A-b	B-b	C-b	D-b	A-c	B-c	C-c	D-c
E_{HOMO}/eV	-8.41	-11.72	-15.31	-19.34	-8.15	-12.43	-15.42	-19.19	-8.69	-12.08	-15.95	-18.67
E_{LUMO}/eV	-0.72	-3.08	-6.53	-10.71	-0.81	-4.10	-7.22	-12.05	-0.36	-3.63	-6.66	-10.04
I/ eV	8.41	11.72	15.13	19.34	7.34	12.43	15.42	19.19	8.69	12.08	15.95	18.67
A/eV	0.72	3.08	6.53	10.71	0.81	4.10	7.22	12.05	0.36	3.69	6.66	10.04
E_{gap}/eV	7.69	8.64	8.78	8.62	8.97	8.32	8.19	7.14	8.32	8.39	9.29	8.63
η/eV	3.84	4.32	4.39	4.31	4.48	4.16	4.09	3.57	4.16	4.19	4.54	4.31
μ/eV	-4.57	-7.40	-10.92	-15.02	-7.66	-8.26	-11.32	-15.62	-4.52	-7.89	-11.31	-14.35
ΔN	1.18	1.71	2.48	3.48	1.75	1.98	2.76	4.37	1.08	1.88	2.43	3.32
E_{FL}/eV	-4.57	7.40-	10.92-	15.02-	-8.55	-8.26	-11.32	-15.62	-4.52	-7.89	-11.31	-14.35
eV /φ	4.57	7.40	10.92	15.02	3.66	8.26	11.32	15.62	4.52	7.89	11.31	14.35

The calculated results indicate that the gap energy value of B12N12 nanocage reduces significantly from pure state with functionalizing nH$^+$ ions, therefore, the conductivity of nanocage increases. Comparison results demonstrate that the gap energy of the A-a to D-c adsorption models alter in range 7.14 to 9.29 eV. It is notable that with adsorbing 5-FC molecule, the gap energy of the B12N12 nanocage decreases significantly from the original state, and so the electric conductivity of nanocage according to $\boldsymbol{\delta \propto e^{-E_{gap}/2KT}}$ increase from the original state and this property is favorable to make the sensitive sensor for detecting 5-FC drugs. A close inspection of results indicates that the electrochemical potential (μ) values of all adsorption models are negative and complex between 5-FC drug and nanocage is stable, and with functionalizing nH$^+$ the stability of system increase with increase the number of H$^+$ ions. The global hardness parameter (η) of the system is in range 3.57 to 4.54 eV. Comparison results denote that the global hardness of 5-FC/B12N12 complex in the **a** and **c** orientations of 5-FC increases slightly with an increasing number of H$^+$ functionalized, whereas in the **b** orientation of 5-FC it decreases slightly with increasing number of nH$^+$ ion functionalized.

The total charge transfer parameters (ΔN) values for all adsorption models are positive. The positive values of ΔN indicate that the charge transfer occurs from the 5-FC drug toward the nanocage surface. Comparison results confirm that the capability of accepting electron charge of nanocage increases with increasing the number of H$^+$ functionalized. The required minimum energy to remove one electron from the Fermi level of a substance is named work function. The work function is calculated by: $\boldsymbol{\varphi = V_{el(\infty)} - E_{FL}}$; the $V_{el(\infty)}$is the electrostatic potential energy of the electron far from the surface of the material which is equal zero, and E_{FL} is Fermi level energy. According to the Richardson & Dushman equation [60], the electron current density (ECD) emitted from the surface of substance (j) will be related to the work function (φ): $\boldsymbol{j = AT^2 e^{-\varphi/KT}}$, where A is Richardson constant (A/m^2) and T is the temperature (K). The work function of nanocage with adsorbing 5-FC and functionalizing nH$^+$ ions increases significantly from the pristine model and so the ECD values of system decrease from original values.

3.3 Quantum theory of atom in molecule (QTAIM) and reduced density gradient (RDG)

By using Bader theory [61] the topological parameters such as total electronic density (ρ), Laplacian of electron densities ($\bigtriangledown^2\rho$), the kinetic energy (G_{BCP}), the total electronic energy (H_{BCP}), the potential energy (V_{BCP}), and ellipticity (ε) at the bond critical point (BCP) of 5-FC…B12N12 nanocage are calculated, and results are given in Table 3 and are shown in Figure S4. Based on the AIM theory, the $\bigtriangledown^2\rho>0$ and $H_{BCP}>0$ denote the weak covalent interactions (strong electrostatic bond), the $\bigtriangledown^2\rho<0$ and $H_{BCP}<0$ values indicate a strong covalent bond, the $H_{BCP}<0$ and $\bigtriangledown^2\rho>0$ denote the medium strength or partially covalent bond. According to results of Table 3, the $\bigtriangledown^2\rho$ values of all adsorption models are positive, whereas the H_{BCP} values of the A-b, D-a and D-b models are positive, and this result shows that the bond between drug and nanocage is strong electrostatic type, and on other models the H_{BCP} values are negative.

This result confirms that the binding between nanocage and 5-FC drug is partially covalent type. The ellipticity values for all adsorption models are in

range 0.0034 to 0.8114 a.u. and the ε is <1. This result demonstrates that the bond between the 5-FC drug and B12N12 nanocage is a sigma bond type. Electron localization function (ELF) is one of the important tools that are used to analyze covalent bonding. If the ELF value is between 0.5 and 1, it indicates regions containing bonding and nonbonding localized electron, when the value of ELF is lower than 0.5 reveals that the electron is delocalized.

Comparison results denote that in the A-a, D-a and D-b models the values of EFL is between 0.5 to 1.0, and this result confirms that the electron density between drug and nanocage is delocalized, and on the other models the values of ELF are lower than 0.5 and that indicates the interaction between drug and nanocage is partially covalent.

For further understanding of the nature of bonding between 5-FC drugs with pristine and nH$^+$ functionalized B12N12, the reduced density gradient (RDG) [62] plots are calculated for all adsorption models. In this method, the product between electron density ρ(r) and the sign of the second-lowest eigenvalues of electron density hessian matrix (λ_2) has been suggested as a tool to distinguish the different types of interactions. The scatter graphs of RDG versus sign (λ_2) ρ(r) for the A-a to D-c models are shown in Fig.5.

In this graph if the sign(λ_2)ρ(r) is 0 (green circle), <0 (blue circle) and >0 (red circle), it represents the interaction between drug and nanocage is van der Walls, hydrogen or covalent attractive and strong repulsive respectively.

Table 3. The Topological parameters (a.u.) of B12N12/5-FC complex for A-a to D-c models

Model	**A-a**	**B-a**	**C-a**	**D-a**
H(r)	-0.2070	-0.3163	-0.4068	0.5875
G(r)	0.1521	0.5308	0.3098	0.2278
V(r)	-0.1728	-0.8471	-0.3505	-0.1302
$\nabla^2\rho$	0.525	0.8577	0.1076	0.5427
ELF	0.7311	0.1561	0.2263	0.5947
ε	0.3829	0.9011	0.0034	0.1720
ρ	0.2013	0.5499	0.4568	0.1670
	A-b	**B-b**	**C-b**	**D-b**
H(r)	0.1214	-0.8457	-0.9831	0.7587
G(r)	0.6135	0.1556	0.1683	0.1278
V(r)	-0.4920	-0.2402	-0.2666	-0.1202
$\nabla^2\rho$	0.2940	0.2842	0.2799	0.5417
ELF	0.2183	0.2201	0.2515	0.5847
ε	0.8114	0.1305	0.0560	0.1759
ρ	0.7997	0.1190	0.1314	0.1687
	A-c	**B-c**	**C-c**	**D-c**
H(r)	-0.3530	-0.8429	-0.1655	-0.8980
G(r)	0.3581	0.1287	0.2695	0.2309
V(r)	-0.3934	-0.2129	-0.4351	-0.2398
$\nabla^2\rho$	0.1291	0.1776	0.4163	0.8880
ELF	0.2003	0.2410	0.3070	0.1261
ε	0.0385	0.0384	0.0550	0.0066
ρ	0.4756	0.1100	0.1894	0.3098

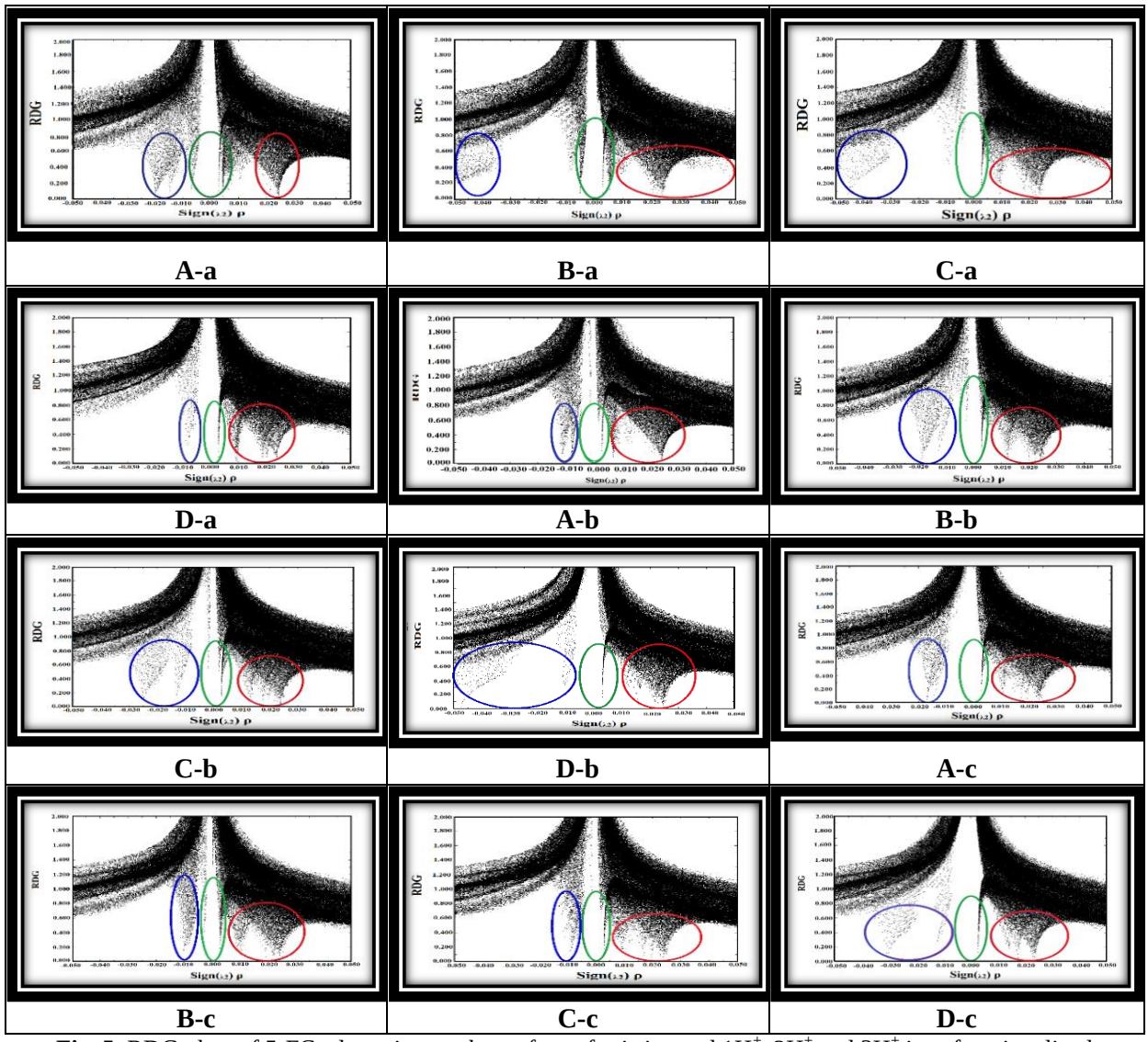

Fig. 5. RDG plots of 5-FC adsorption on the surface of pristine and $1H^+$, $2H^+$ and $3H^+$ ions functionalized B12N12 nanocage (A-a to D-d), models.

Comparison results indicate that in the A-a to D-c models the most electron density of RDG is localized in the $\lambda_2<0$ region and the attractive interactions between 5-FC drug with nanocage is more than other models. This result confirms that the interaction between 5-FC with B12N12 is noncovalent and it is in agreement with QTAIM and ELF results.

3.4 Excited-state and UV-visible and none linear optical (NLO) properties

For better investigating the optical property of the system and determining the fluorescence, UV-visible spectrum and excited state of a molecule, the TD-DFT method at the WB97XD/6-31G (d, p) level of theory is applied for 20 excited states [63], and the transition of electron results for all studied models are listed in Table S3 (in supplementary data) and the Uv-visible spectrum is displayed in Figure 6.

As can be seen from Fig. 6, the highest UV absorption intensity for A-a, B-a, C-a, and D-a has occurred in λ_{max} of 176.46 ($S_0 \rightarrow S_{17}$), 177.5 ($S_0 \rightarrow S_{21}$), 173.69 ($S_0 \rightarrow S_{25}$) and 180.49 ($S_0 \rightarrow S_{17}$) nm respectively, and for A-b, B-b, C-b, and D-

b have observed in λ_{max} of 173.61 ($S_0 \rightarrow S_{20}$), 169.94 ($S_0 \rightarrow S_{25}$), 184.82 ($S_0 \rightarrow S_{24}$) and 178.03 nm ($S_0 \rightarrow S_{28}$) respectively, and for A-c, B-c, C-c and D-c has observed in λ_{max} of 174.43($S_0 \rightarrow S_{28}$), 171.11 ($S_0 \rightarrow S_{25}$), 168.69 ($S_0 \rightarrow S_{21}$) and 179.75 nm ($S_0 \rightarrow S_{16}$) respectively. This result reveals that the λ_{max} of all models is in the ultraviolet region. To investigate the nonlinear optical properties of the molecule the Polarizability (α_0) and first hyperpolarizability (β_0) parameters are calculated and results are listed in Table 4.

The polarizability and hyperpolarizability are favorable parameters in the design of optoelectronic devices, optical switching, signal processing, and terahertz wave generation [64–65]. The β_0 is associated with intramolecular charge transfer resulting from an electron donor to electron acceptor groups.

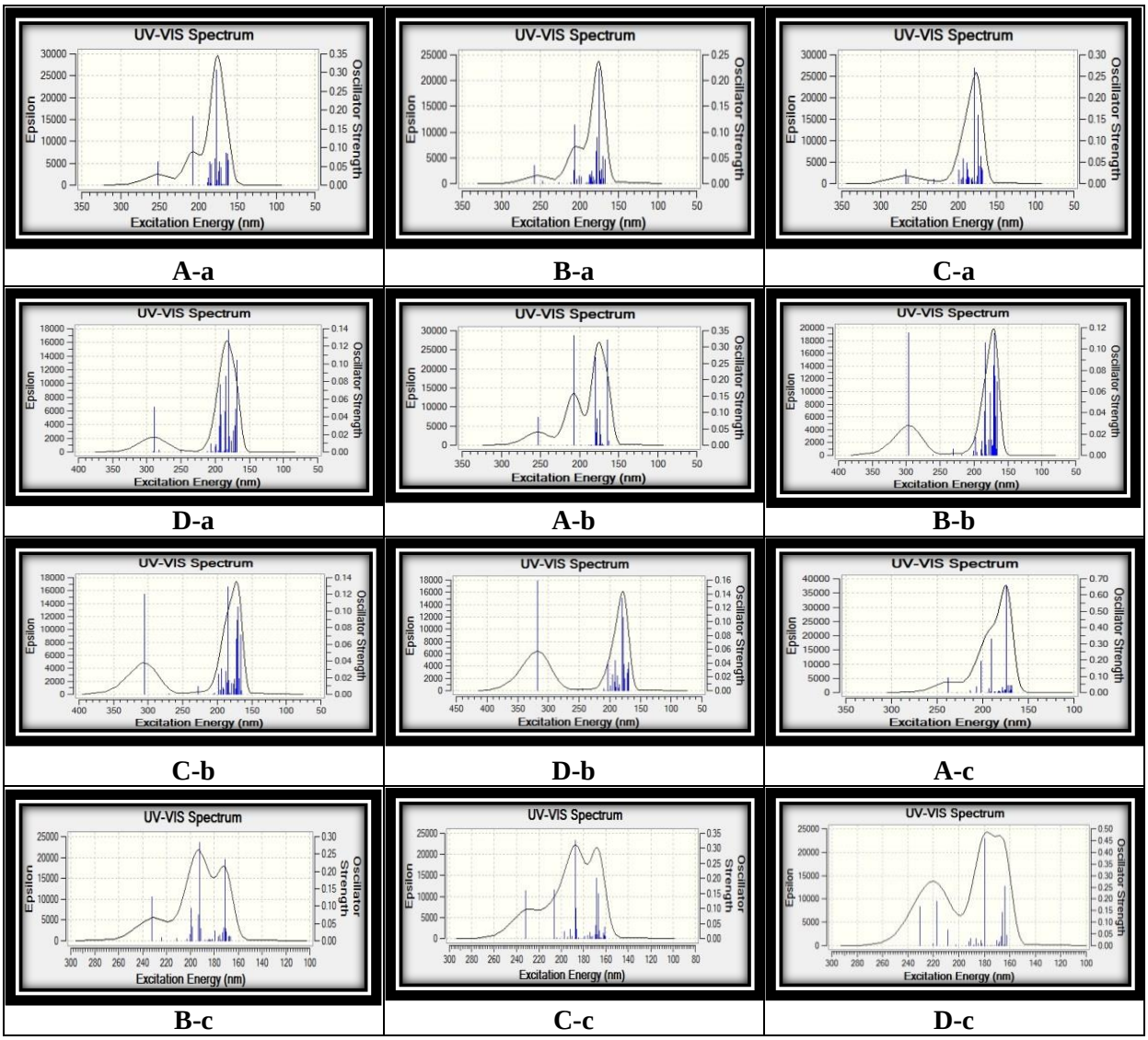

Fig. 6. Uv-visible plots of 5-FC adsorption on the surface of pristine and $1H^+$, $2H^+$ and $3H^+$ ions functionalized B12N12 nanocage (A-a to D-d), models.

Table 4. The Total polarizability (α_0 /a.u.) and hyperpolarizibility (β_0/ a.u.), dipole moment (μ /debye) B12N12/5 -FC complex for A-a to D-c models

Model	α_o	β_0	μ
A-a	204.97	256.00	1.87
B-a	202.30	240.53	3.10
C-a	205.17	304.40	3.02
D-a	205.90	260.68	4.11
A-b	207.48	160.08	2.21
B-b	202.53	132.37	3.55
C-b	202.99	42.18	3.81
D-b	205.09	603.98	7.31
A-c	214.34	202.62	5.00
B-c	205.47	124.44	5.58
C-c	205.34	103.11	5.17
D-c	206.79	90.82	4.38

Comparison results indicate that the α_0 values of all adsorption models are in range 202.30 to 214.34 a.u., whereas the values of β_0 for all adsorption models are in range 42.18 to 603.98 a.u. The results demonstrate that the hyperpolarizability value of the D-b model is more than the other model and this model has a more optical property. Dipole moment of all adsorption models are in the range of 1.87 to 7.31 debye, and the interesting point is that with an increasing number of functionalized $n\mathrm{H}^+$ ions, the dipole moment of nanocage increases, and so the binding drug on the surface of nanocage increase.

4. CONCLUSIONS

In the current study, the structural, electrical, quantum parameters, thermodynamic parameters, solvent effect, AIM, RDG, UV-visible spectrum, and Polarizability (α_0) and first hyperpolarizability (β_0) parameters for adsorption of 5-FC on the surface of pristine and $n\mathrm{H}^+$ functionalized B12N12 are calculated. The order of increasing adsorption of 5-FC drug in different drug positions on the surface of pristine B12N12 nanocage is as follows: **c** (−37.46 kcal/mol)>**d** (−12.37 kcal/mol)>**a**(−10.31 kcal/mol)>**b**(−5.17 kcal/mol) and this result demonstrates that adsorption drug from O head is more favorable than other position. It is notable than with an increasing number of H^+ the adsorption energy of 5-FC increases.

The Gibbs free energy results reveal that the formation of 5-FC/nanocage complex in the gaseous and solution phase is unspontaneous and spontaneous respectively. The electrochemical potential (μ) values of all adsorption models indicate that a bonding between 5-FC drug and nanocage is stable, and with functionalizing H^+ ion the stability of system increase with increasing the number of H^+ ions. The work function of nanocage with adsorbing 5-FC and functionalizing $n\mathrm{H}^+$ ions increases significantly from pristine states and so the ECD values of system decrease from original values. The results of RDG, AIM and ELF result confirms that the interaction between 5-FC with B12N12 is noncovalent. The dipole moment of all adsorption models with an increasing number of H^+ functionalized increases, and so the bonding drug on the surface of nanocage increases, this result is useful to make a carrier and deliver of drug in biological.

Supplementary data

Tables S1- S3 and Figures S1- S4 are given in supplementary data.

REFERENCES

[1] M. K. Hazrati, Z. Javanshir, Z. Bagheri, J. Mol. Graph .77 (2017) 17–24.

[2] A. Bahrami, S. Seidi, T. Baheri, M. A. Aghamohammadi, Superlat. Microst. 64(2013) 265–273.

[3] M. B. Javan, A .Soltani, Z. Azmoodeh, N. Abdolahi, N. A. Gholami, RSC. Adv. 6(106) (2016) 104513–104521.

[4] A. S. Rad, K. Ayub, J. Alloys. Comp. 672 (2016) 161–169.

[5] M. B. Javan, A. Soltani, E. T. Lemeski, A. Ahmadi, A. S. Rad, Superlatt. Microst. 100 (2016) 24–37.

[6] T. Oku, A. Nishiwaki, I. Narita, Sci. Technol. Adv Mat.5 (2004) 635–645.

[7] [7] J. Beheshtian, Z. Bagheri, M. Kamfiroozi, A. Ahmadi, J. Mol. Model. 18 (2012) 2653–2658.

[8] S. Xu, M. Zhang, Y. Zhao, B. Chen, J. Zhang, C.C. Sun , Chem. Phys. Lett. 423(2006) 212–214.

[9] R. Rahimi1, M. Solimannejad, Str. Chem. 30 (2019) 979–987.

[10] A. V, Pokropivny, Diamond. Related. Mat. 15(2006) 1492 – 1495.

[11] Z. Zhao, Z. Li, Q. Wang, Chem. Phy. Lett. 739(2020) 136922.

[12] E. Shakerzadeh, N. Barazesh, S. Zargar Talebi, Superlatt. Microstr. 76 (2014) 264–276.

[13] S. Yourdkhani, T. Korona, N. L. Hadipour, J. Phys. Chem. A. 119 (2015) 6446–6467.

[14] H. Wu, X. Fan, J.-L. Kuo, Int. J. Hydrog. Energy. 37(2012) 14336–14342.

[15] F. Zhao, Y. Wang, M. Zhu, L Kang, RSC. Adv. 5 (2015) 56348–56355.

[16] M. D. Esrafili, R. Nurazar, Comp. Mate. Sci. 92 (2014) 172–177.

[17] M. D. Esrafili, R. Nurazar, J. Clust. Sci. 26 (2015) 595–608.

[18] E. Vessally, E. Ahmadi, M. D. Esrafili, A. Hosseinian, Monatsh. Chem. 148 (2017) 1727–1731.

[19] A. S. Rad, Semiconduct. 51 (2017) 134–138.

[20] A. A. Peyghan, H. Soleymanabadi, Cur. Sci. 108 (2015) 00113891–00113901.

[21] E. Vessally, S. Soleimani-Amiri, A. Hosseinian, L. Edjlali, A. Bekhradniae, Physica E. 8 (2017) 308–311.

[22] D. Quiñonero, A. Frontera, P. M. Deyà, J. Phys. Chem. C. 116 (2012) 21083–21092

[23] M. T. Baei, Heteroat. Chem. 24 (2013) 476–481

[24] P. Fallahi, H. Jouypazadeh, H. Farrokhpour, J. Mol. Liq. 260 (2018) 138–148

[25] M. Noei, Vacuum. 135 (2017) 44-49

[26] E. Tazikeh‑Lemeski, A. Soltani, M. T. Baei, M. B. Javan, S. Moazen Rad, Adsorption. 24 (2018) 585–593.

[27] R. Padash, M. Rahimi-asrabadi, A. S. Rad, A. Sobhani-Nasab, T. Jesionowski, H. Ehrlich, J. Clust. Sci, 30 (2019) 203–218.

[28] E. Shakerzadeh, Physica E. 78 (2016) 1–9.

[29] M. T. Baei, Comp. Theo. Chem. 1024 (2013) 28–33.

[30] F. Rahimi, A. Zabaradsti, J. Inorg. Organomet. Polym. 27(2017) 1770–1777.

[31] R. Pino-Rios, E. Chigo-Anota, E. Shakerzadeh, G. Cardenas-Jiron, Physica E. 115 (2020) 113697.

[32] E. Vessally, F. Behmagham, B. Massuomi, A. Hosseinian, K. Nejati, J. Mol. Model. 23(2017) 138-145.

[33] A. S. Rad, K. Ayub, Ineter. J. hydrogen energy. 41 (2016) 22182–22191.

[34] R. Rahimi, M. Solimannejad, Struct. Chem. 31 (2020) 447–454.
[35] M. D. Esrafili, R. Nurazar, Superlat. Microstr. 67 (2014) 54–60.
[36] A. Soltani, M.T. Baei, E. Tazikeh Lemeski, A. A. Pahlevani, Superlat. Microstr. 75 (2014) 716–724.
[37] A. S. Ghasemi, A. Soltani, M. Karimnia, F. Ashrafi, F. Heidari, M. Majidian, J. Mol. Liq. 277 (2019) 115–122.
[38] D. Farmanzadeh, M. Keyhanian, Theo. Chem. Accounts. 138 (2019) 11
[39] R. Padash, A. Sobhani‐Nasab, M. Rahimi‐Nasrabadi, M. Mirmotahari, H. Ehrlich, A. S. Rad, M. Peyravi, Appl. Phys. A. 124 (2018)582–590.
[40] H. Zhu, C. Zhao, Q. Cai, X. Fu, F. R. Sheykhahmad, Inorganic Chem. Comm. 114 (2020) 107808.
[41] M. T. Baei, M. Ramezani Taghartapeh, E. Tazikeh Lemeski, A. Soltani, Physica B. 444 (2014) 6–13.
[42] A. Bahrami, S. Seidi, T. Baheri, M. Aghamohammadi, Superlat. Microstr. 64 (2013) 265–273.
[43] S. Larki, E. Shakerzadeh, E. Chigo Anota, R. Behjatmanesh-Ardakani, Chem. Phy. 526 (2019) 110424.
[44] C. Heidelberger, L. Griesbach, B. J. Montag, D. Mooren, O. Cruz , R. J. Schnitzer, et al.. Cancer. Res. 18 (1958) 305–317
[45] E. Grunberg, E. Titsworth, M. Bennett, Antimicro. Agents. Chemotherapy. 3(1963) 566–568.
[46] D. Tassel, M. A. Madoff, J. American Med. Assoc. 206 (1968) 830–832.
[47] J. M. Benson, M. C. Nahata, Clinical Pharmacy. 7 (1988) 424–438.
[48] M. P. Deonarain, R. A. Spooner, A. A. Epenetos, Gene Therapy. 2(1995) 235–44.
[49] M. J. Frisch, et al. Gaussian 09, Revision, Gaussian, Inc., Wallingford CT. (2009).
[50] R. G. Parr, L.V. Szentpaly, S. Liu, J. Am. Chem. Soc. 121(1999) 1922–1924.
[51] R. G. Pearson, PNAS-USA, 83 (22) (1986) 8440–8441.
[52] M. Rezaei-Sameti, H.J. Behbahani, Phys. Chem. Res., 6(2018) 31–43.
[53] M. Rezaei-Sameti, B. Amirian , Asian J. Nanosci. Mate. 1(4) (2018) 262−270
[54] J. Padmanabhan, R. Parthasarathi, V. Subramanian, P. K. Chattaraj, J. Phys. Chem. A 111 (2007) 1358–1361.
[55] M. Rezaei-Sameti, S. K. Abdoli, J. Mole. Stru. 1205(2020)127593.
[56] M. Rezaei‐Sameti, P. Zarei, Adsorption, 24 (8) (2018) 757−767.
[57] M. Rakhshi, M. Mohsennia , H. Rasa , M. Rezaei Sameti, Vacuum. 155 (2018) 456–464.
[58] M. D. Esrafili, Physics Lett. A. 381 (2017) 2085–2091.
[59] B. Mennucci, Wiley Interdiscip. Polarizable continuum model, Rev.: Comput. Mol. Sci. 2 (2012) 386–404.
[60] O. Richardson, Phys. Rev. 23 (1924) 153–157.
[61] R. F.W. Bader, Atoms in Molecules: A Quantum Theory, Oxford University Press, Oxford, U.K. (1990)
[62] T. Lu, F. Chen, J. Comput. Chem. 33 (2012) 580−592.
[63] Y. T. Sun, P.Y. Huang, C. H. Lin, K. R. Lee, M. T. Lee, Biophys. J. 110 (2015) 414–418.
[64] F. Kajzar, K.S. Lee, A. K. Y. Jen, Adv. Polym. Sci. 161(2003)1−85.
[65] V. Krishnakumar, R. Nagalakshmi, Physica B. 403 (2008) 1863−1869.